Journal of Neuroscience Methods 417 (2025) 110391

Contents lists available at ScienceDirect

Journal of Neuroscience Methods

journal homepage: www.elsevier.com/locate/jneumeth

Integration of focused ultrasound and dynamic imaging control system for targeted neuro-modulation

K.M. Karthick Raghunath [a], Surbhi Bhatia Khan [b,h,i,*], T.R. Mahesh [a], Ahlam Almusharraf [c], Rubal Jeet [d], Mohammad Tabrez Quasim [e], Azeem Irshad [f], Fatima Asiri [g]

[a] Department of Computer Science and Engineering, Faculty of Engineering and Technology, JAIN (Deemed-to-be University), Bangalore 562112, India
[b] School of science, engineering and environment, University of Salford, United Kingdom
[c] Department of Management, College of Business Administration, Princess Nourah Bint Abdulrahman University, P.O. Box 84428, Riyadh 11671, Saudi Arabia
[d] Chandigarh Engineering College,Jhanjeri, Mohali, Punjab, India
[e] Department of Computer Science and Artificial Intelligence, College of Computing and Information Technology, University of Bisha, P.O Box 551, Bisha, Saudi Arabia
[f] GGC Asghar Mall, HED, Rawalpindi, Punjab, Pakistan
[g] College of Computer Science, Informatics and Computer Systems Department, King Khalid University, Saudi Arabia
[h] University Centre for Research and Development, Chandigarh University, Mohali, Punjab, India
[i] Centre for Research Impact and Outcome, Chitkara University Institute of Engineering and Technology, Chitkara University, Rajpura, 140401, Punjab, India

ARTICLE INFO

Keywords:
FMRI
NIRS
Brain
Neuro-modulation
Simulation
Non-invasive
Closed loop
Targeting accuracy
Therapeutic
TFUS

ABSTRACT

Background: Transcranial Direct Current Stimulation (tDCS) and Transcranial Magnetic Stimulation (tMS) have received widespread clinical use as techniques within a Non-Invasive Brain Stimulation (NIBS) domain, whose primary focus is modulation of neural activity to treat neurological and psychiatric disorders. Despite these advancements, precision targeting of deep brain structures remains a challenge faced with great need of another innovation that will improve precision and reduce the risks. A novel methodology integrating transcranial Focused Ultrasound (tFUS) with real-time functional imaging modalities, including functional Magnetic Resonance Imaging (fMRI) and Near-Infra-Red Spectroscopy (NIRS), is proposed in this study as the Integrated Focused Ultrasound and Real-Time Imaging Control System (IFURTICS).
Principle results: Closed loop algorithms employed by IFURTICS allow it to dynamically vary stimulation parameters in response to real-time feedback on neural activity, allowing for accurate targeting of sensitive networks while minimizing deleterious collateral effects.
Conclusions: Clinical trials using standard datasets of fMRI and NIRS have proved that the approach improved targeting accuracy by ~18 %, reduced off-target effects by ~55 % and enhanced therapeutic outcomes by 50 % over current methods, suggesting its potential as a transformative approach to precision neuro-modulation.

1. Introduction

Transcranial Magnetic Stimulation (TMS), however, Transcranial Direct Current Stimulation (tDCS), and Transcranial Focused Ultrasound (tFUS) are non-invasive brain stimulation modalities as tools to modulate neural activity in a rapidly developing field (Darmani et al., 2022). Selectively targeting defined brain regions to influence cortical and sub-cortical activity is aimed at treating a number of neurological and psychiatric disorders with these technologies. Non-Invasive Brain Stimulation (NIBS) is based on physical principles (such as electromagnetic fields or acoustic waves), which can be used in neuro-modulatory action without surgical operation. NIBS is an essential tool in neuroscience and clinical neuro-engineering, and its applications span major disorders, including depression, epilepsy, Parkinson's disease and cognitive impairments (Wang et al., 2023).

NIBS lie at the intersection of neuroscience, biomedical engineering, and computational modeling to build brain-targeted approaches to manipulate brain activity. Increasingly, both Near-Infrared Spectroscopy (NIRS) and functional MRI (fMRI), as means of advanced imaging, have been incorporated into NIBS to offer real-time feedback for

* Corresponding author at: School of science, engineering and environment, University of Salford, United Kingdom.
E-mail addresses: karthick.km@jainuniversity.ac.in (K.M. Karthick Raghunath), s.khan138@salford.ac.uk (S.B. Khan), trmahesh.1978@gmail.com (T.R. Mahesh), aialmusharraf@pnu.edu.sa (A. Almusharraf), rubal.j2932@cgc.ac.in (R. Jeet), tabrezquasim@gmail.com (M.T. Quasim), azeemirshad@gpgcam.edu.pk (A. Irshad), Falmalye@kku.edu.sa (F. Asiri).

https://doi.org/10.1016/j.jneumeth.2025.110391
Received 11 December 2024; Received in revised form 20 January 2025; Accepted 8 February 2025
Available online 22 February 2025

precision targeting (Curtin et al., 2019; Bergmann et al., 2016). In addition, closed-loop systems and computational techniques have become vital in improving the safety, adaptability and therapeutic efficacy of these interventions (Zhao et al., 2024; Pu et al., 2024). This domain has altered the path of treatment paradigms from invasive procedures (deep brain stimulation [DBS]) to safer and patient-friendly modalities (Williams and Okun, 2013). The combination of hardware improvements, technical progressions and neuro-physiological understanding drives the evolution of NIBS as an essential component of personalized medicine.

In this study, the Integrated Focused Ultrasound and Real-Time Imaging Control System (IFURTICS) are proposed as a new framework aimed at mitigating the shortcomings of current NIBS methods. Neuromodulation with high spatial and temporal precision is achieved by combining Transcranial Focused Ultrasound (tFUS) with real-time functional imaging modalities such as fMRI and NIRS (Luan et al., 2023; Yu et al., 2023) in IFURTICS. The framework uses a closed-loop feedback process to adjust stimulation parameters dynamically and continuously by monitoring neural responses. The optimization engine underlying this system is a core feature and minimizes off-target effects by applying advanced loss functions and regularization techniques to achieve precise alignment of theoretical activation profiles with observed neural patterns. Through the integration of these components, IFURTICS provides the clinic with the elements of an innovative clinical strategy for the successful treatment of complex neurological and psychiatric conditions.

The brain is of utmost future research significance in this domain since the brain is able to precisely and non-invasively target complex and deep brain structures, which is fundamental for treating neurological and psychiatric disorders (Tarazi and Schetz, 2005). This approach enables any studies of the complex neural networks in the brain while, in one fell swoop, ensuring safety and minimization of side effects of precision neuro-modulation. Fig. 1 depicts some of the vital brain sections that need to be considered for the research because they hold key sites of involvement in neurological and psychiatric disorders targeted by NIBS (Alfihed et al., 2024; Edelman et al., 2015). Unlike the other parts of the brain, the Prefrontal Cortex plays a major role in decision-making, emotion, and executive functions, and so is, say, number one for depression and anxiety. The thalamus functions as a relay centre between the sensory and motor signal systems, and this is important to understand in disorders such as epilepsy and Parkinson's disease (Parnaudeau et al., 2018). Likewise, the Hippocampus and Amygdala sustain fundamental memory and emotional regulation and bear on PTSD and Alzheimer's (Hanson et al., 2015). The Basal Ganglia (Favila et al., 2024) is centrally involved in motor control and is extremely implicated in movement disorders. Voluntary movements and sensory processing vital to conditions such as stroke rehabilitation are directly linked to Motor Cortex and Somatosensory Cortex (Kim et al., 2024), respectively. The functions of the anterior portion of the Cingulate Cortex (Alejandro and Holroyd, 2024) reveal that it plays a major role in emotional and attentional regulation, and dysfunction may contribute to disorders and chronic pain. Lastly, the ventricles are important for cerebral spinal fluid dynamics, and they also indirectly affect brain health because they are reference points for performing accurate deep brain targeting. As a group, those areas constitute the anatomical and functional basis on which precise and efficient neuro-modulation strategies can be designed in the study.

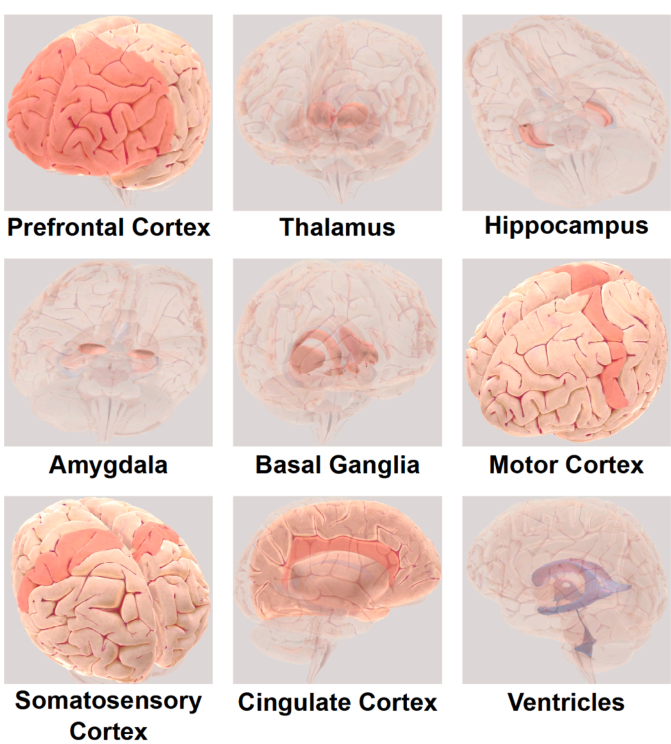

Fig. 1. Vital Region of Brian for Investigation via IFURTICS.

1.1. Research significance

This work is significant because it sets forth a path to transforming this field of non-invasive neuro-modulation by tackling these critical technical and clinical challenges. Real-time image feedback integration enables adaptive and precise targeting of deep brain structures, thus minimizing off-target effects. Not only does this adaptability improve therapeutic outcomes, but it also expands the area in which NIBS can be applied to hitherto inaccessible areas of the brain. Additionally, the closed-loop system provides unprecedented safety, continuously monitoring and correcting based on each participant's neural response. Further, the proposed framework provides a robust computational basis for future work in scaling and integration of personalized neuromodulation therapies (Kar and Vidya, 2023) with clinical workflows.

1.2. Scope and motivation

This research aims to develop a new patient-centric neuro-modulation framework to address a wide range of neurological and psychiatric disorders encompassing depression, epilepsy, Parkinson's disease, and Alzheimer's disease (Chen et al., 2023). Based on the predefined contribution, IFURTICS can also be used to understand neuro-physiological mechanisms underlying such conditions by employing real-time functional imaging and adaptive algorithms. This study is motivated by the lack of precision, safety, and efficacy with regard to neuro-modulation, as well as the promise of NIBS to revolutionize global healthcare with the potential for noninvasive and scalable treatments. As such, this research spans an interdisciplinary domain, including neuroscience, biomedical engineering, and computational modeling—a foundational advancement in neuro-therapeutics.

1.3. Research novelty

The important innovation in this work is the development and integration of the IFURTICS, providing unprecedented precision and flexibility of noninvasive brain stimulation. Rather than relying on traditional NIBS methods that utilize large transcranial current stimulation configurations for low spatial resolution, IFURTICS uses tFUS for high spatial resolution and utilizes the real-time functional imaging modalities fMRI and NIRS to monitor neural activity during stimulation in real-time. A closed-loop feedback procedure is introduced to continuously adjust the stimulation parameters with respect to real-time neural responses to accommodate individual variability as well as to minimize the off-target effects. Moreover, the framework provides an optimization engine to coarsely align theoretically and observed neural activation profiles with advanced computational loss functions to guarantee accuracy and safety. The combination of adaptive imaging, closed-loop control, and computational optimization in this novel manner establishes a new transformative platform that can improve outcomes of therapy, extend the applicability of NIBS to deep structures in the brain, and set a new benchmark for precision neuro-modulation in personalized medicine.

Finally, the study presents the IFURTICS framework, which fuses real-time functional imaging methods such as fMRI and NIRS with closed-loop feedback in order to perform closed-loop dynamic and adaptable stimulation. This work constitutes a significant contribution towards the advancement of precision neuro-modulation and the following descriptions highlight those contributions for better understanding.

- Temporal modulation factors are optimized to address critical challenges in targeting accuracy, off-target effects and therapeutic efficacy, and encoding temporal computerized representations of molecular pharmacology are utilized to gain advantages of high selectivity and in vivo efficacy.
- The framework establishes a benchmark for coupling imaging and stimulation technologies for applications in which precise spatial and temporal control of neuro-modulation is desired.
- Furthermore, by using standard fMRI and NIRS datasets, we obtain rigorous validation and applicability over a wide range of neurological and psychiatric disorders.
- In addition, this work can start to shed light on neuroengineering, computational neuroscience and clinical applications to enable interdisciplinary advancements and future developments in targeted therapies through this work.

2. Relevant studies

In (Qiu et al., 2017), a portable ultrasound system for non-invasive neuro-stimulation was employed using a miniaturized PMN-PT (1–3 composite single crystal, Lead Magnesium Niobate-Lead Titanate) transducer and programmable waveform generator. In-vivo and in-vitro neuro-modulation was demonstrated in the system with up to 13 % improvement in intensity over current PZT transducers and reliable stimulation of mouse brain and retinal ganglion cells. However, this method is currently incompatible with MRI-guided uses, and further refinement is required to accommodate multi-site stimulation situations. In Li et al. (2018), Imaging-guided Dual-target Neuro-modulation System (IDNS) via array ultrasound was used to provide precise non-invasive stimulation of multiple brain regions in mice. They demonstrated that with significant success, it showed selective responses between two distinct brain targets with a significant 73 per cent attenuation in acoustic intensity through the skull barrier, and hence, it allowed the system to navigate towards targets reliably. Limitations include a reliance on models that are not directly applied to humans and the need for additional evaluation of long-term safety and neuro-modulatory effects.FUS displacement imaging coupled with high frame rate ultrasound and GPU acceleration was used by Lee et al. (2020) to apply non-invasive neuro-modulation of the median nerve for pain relief. Initial human trials demonstrated promising real-time targeting and feedback capabilities, and it achieved up to 50.1 microns cumulative nerve displacement and a 0.96 pain rating unit decrease in thermal pain perception. However, there is variability in displacement across subjects due to the coupling and the tissue differences, as well as the need for broader clinical trials to establish efficacy and safety. To explore a non-invasive approach to the use of neuro-modulation for epilepsy treatment, Lin et al. (2020) used low-intensity pulsed ultrasound (LIPUS) while relying on electrophysiology, immune-histochemistry and behavioral analysis. Balancing excitatory and inhibitory synaptic inputs achieved a 39 % reduction in total seizure count and greater than 65 % inhibition of epileptic form discharges in human epileptic tissues. Limitations are that therapeutic effects are based on animal models or human tissue slices rather than full-scale clinical trials, leading to concerns about the scalability and consistency of therapeutic effects. The study in Schafer et al. (2020) used Low-Intensity Focused Ultrasound Pulsation (LIFUP) in an MRI-safe system (650 kHz transducer) to demonstrate non-invasive neuro-modulation for use in brain mapping and therapeutic applications. Significant advancements were made, including an 85 % reduction in system weight and size with peak pressure of up to 3.8 MPa at the focal point, which allowed for precise stimulation. However, dependency on accurate skull and tissue calibration and broader clinical validation for diverse patient populations remains a limitation. A spatial multi-target ultrasound neuro-modulation system based on a high-powered 2D array transducer was developed in Zhuang et al. (2022) as a platform for non-invasive multi-target neuro-modulation in small animals. The system achieved precise stimulation with a peak acoustic pressure of 2.21 MPa, which is significantly higher than previous systems, and spatial targeting error < 1.5 mm. However, there are limitations, such as difficulty in controlling ultrasound beams at multiple focal lengths and possible alignment errors associated with skull-induced aberrations. Researchers in Yüksel et al. (2023) used non-invasive neuro-modulation to study Low Intensity – FUS (LI–FUS) for stroke recovery. The technology showed highly accurate targeting of deep brain structures and demonstrated up to 30 % improvement in motor function recovery in preclinical models. However, poor standardization across ultrasound parameters and inadequate large-scale human trials restrict generalizability and clinical adoption of the use. In Hsieh et al. (2024), the authors studied one-hour intermittent and continuous tFUS on rats' motor cortex. Motor excitability was assessed with motor evoked potentials (MEPs), and c-Fos and GAD-65 neural biomarkers were determined using immune-histochemistry. Brief facilitation of motor excitability (lasting ~5 min) and increased c-Fos (excitatory marker) were observed in response to intermittent tFUS, resulting in a peak of ~46.9 % enhancement of MEP. Unlike continuous tFUS, which always decreased excitability (MEP inhibition up to ~30 % in addition to increased GAD 65; an inhibitory marker), intermittent and variable length tFUS both elicited significant inhibition and facilitation. Each technique spared the brain (no GFAP elevations). Intermittent tFUS showed transient efficacy, while continuous tFUS displayed sustained suppression; each has its own limit on duration and specificity. Clinical potential is shown, and there is a need for optimized parameterization. Non-invasive neuro-modulation Lee et al. (2024) was used to remotely map cortical hemodynamic responses in mice for the treatment of neuropathic pain using functional ultrasound imaging in conjunction with FUS. The study aimed to correlate FUS-evoked hemodynamics with pain intensity and to show significant modulation of neuropathic pain responses with high-resolution cortical connectivity mapping associated with altered functional connectivity in neuropathic models. Yet limitations include the reliance on animal models without direct human validation and variability of translation of hemodynamic correlations to broader clinical settings.

3. Methodology

The IFURTICS architecture depicted in Fig. 2 is comprised of five core processing modules, all of which are dedicated to precision neuromodulation. The first stage is the tFUS neural modulation module, which produces ultrasound beams spatially and temporally modulated in order to deliver adequate therapy to deep brain regions with high precision by minimizing energy dissipation via pressure wave integrals. Neural activity is captured dynamically — with fMRI or NIRS — by the real-time imaging integration layer, which performs advanced signal processing to improve spatial resolution while minimizing noise. These data are fed into the closed-loop feedback mechanism consisting of adaptive algorithms computing instantaneous adjustments to stimulation parameters

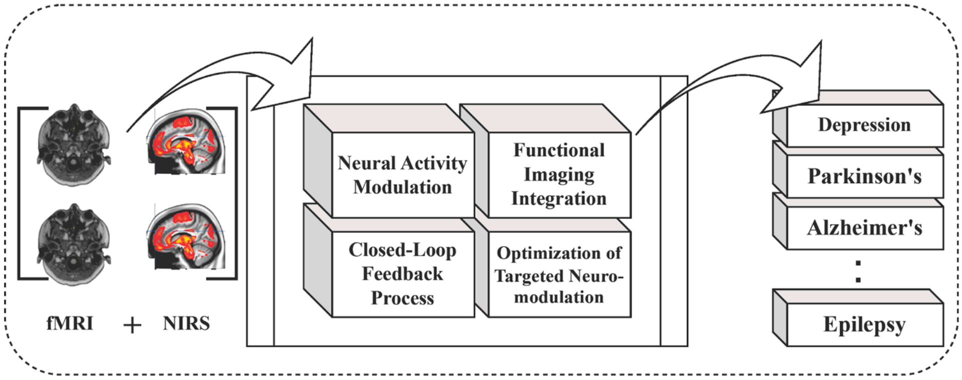

Fig. 2. Architecture of IFURTICS.

based on correlating imaging feedback with neural responses. The optimization engine refines targeting errors and suppresses off-target stimulation using regularized loss functions by aligning theoretical and detected activation profiles. Finally, the therapeutic evaluation module evaluates efficiency by determining the amount of neural activation that was seen during stimulation and comparing that to the amount of stimulation used, enabling neural activation with maximum outcome and minimum collateral effects. The combination of these processes results in a robust, adaptive architecture for precise real-time brain stimulation.

3.1. Neural activity modulation

The tFUS's role is to deliver precisely focused ultrasound energy to a modulate activity of a feed (i.e. to do focused neuro-modulation without opening the skull). Several steps are included in this modulation that comprises the generation of focused ultrasound waves from spatially and temporally modulated beam profiles. Such ultrasound beam profile (Mace et al., 2013) $B(f,\theta)$ is computed on a per target depth/frequency (f) and angle (θ), so as to ensure minimal energy dissipation. Within the beam propagation, as well as gain functions and boundary constraints, the integration over the ultrasound source region R allows for precise focus on the desired neural region while avoiding neighboring structures.

Mathematical expressions for computing any point of induced pressure wave at the target location with contributions from all source elements over the region R are as follows.

Initially the propagation (þ) of sound wave (in medium) is computed as,

$$\nabla^2 \bullet \text{þ}(\boldsymbol{x},\boldsymbol{y},\boldsymbol{z},\boldsymbol{t}) - \partial^2\text{þ}(\boldsymbol{x},\boldsymbol{y},\boldsymbol{z},\boldsymbol{t})/\partial\boldsymbol{t}^2 \bullet \boldsymbol{c}^2 = \boldsymbol{0} \tag{1}$$

Now, the calculation of the propagation of sound in a medium through the Fourier transform of the pressure wave in the frequency domain, $\widehat{\text{þ}}(x,y,z,\omega)$, which is expressed as,

$$\text{þ}(\boldsymbol{x},\boldsymbol{y},\boldsymbol{z},\boldsymbol{t}) = \int_{-\infty}^{\infty} \widehat{\text{þ}}(\boldsymbol{x},\boldsymbol{y},\boldsymbol{z},\omega) \bullet \boldsymbol{e}^{i\omega t}\boldsymbol{d\omega} \tag{2}$$

From temporal modulation, the Harmonic oscillation term ($e^{i\omega t}$) is integrated in Eq. (2). The pressure field is later computed in the frequency domain as,

$$\widehat{\text{þ}}(\boldsymbol{x},\boldsymbol{y},\boldsymbol{z},\omega) = \int_R B(f,\theta) \bullet \text{₲}(\boldsymbol{x},\boldsymbol{y},\boldsymbol{z})\boldsymbol{dR} \tag{3}$$

Eq. (3) aids to represent the beam profile $B(f,\theta)$and propagation gain coordinates $\text{₲}(x,y,z)$ to take into account the ultrasound source contributions that contributes to the final pressure wave at the target, which is expressed as,

$$\text{þ}(\boldsymbol{x},\boldsymbol{y},\boldsymbol{z},\boldsymbol{t}) = \int_R \boldsymbol{B}(\boldsymbol{f},\boldsymbol{\theta}) \bullet \text{₲}(\boldsymbol{x},\boldsymbol{y},\boldsymbol{z}) \bullet \boldsymbol{e}^{i\omega t}\boldsymbol{dR} \tag{4}$$

These computations are composed to build a progressive basis from which the final representation of the pressure wave is formed. Thus, during the final computation of the pressure wave at the target, the energy is delivered accurately, which forms the basis of real-time imaging feedback for dynamic monitoring and regulating the stimulation parameters in the following steps.

3.2. Functional imaging integration (FII)

In the case of tFUS, neural responses are measured in functional imaging data in real time (i.e fMRI or NIRS) while acquiring tFUS application. Further, this scheme is governed by an intensity function that incorporates spatial frequency (τ), noise reduction, and temporal dynamics, producing high fidelity records of subtle neural modulations (Mitra and Pesaran, 1999). Adaptive techniques adapt the kernel $\text{Ɽ}(x)$ to decimate noise and enhance signal clearness.

The computational procedure of this imaging integration involves signal dynamic processing acquired from neural modulation and estimating resolution matrix for spatial and contrast characteristics.

The hemodynamic response $\text{ɦ}(x,y,z,t)$is integrated over the stimulated section (φ) and assigned a weightage via a spatial sensitivity,$S_\omega(x,y,z)$, thus deriving dynamics of neural activity signal$\left(D_{\sigma(t)}\right)$ as,

$$\boldsymbol{D}_{\sigma(t)} = \int_\varphi \boldsymbol{S}_\omega(\boldsymbol{x},\boldsymbol{y},\boldsymbol{z}) \bullet \text{ɦ}(\boldsymbol{x},\boldsymbol{y},\boldsymbol{z},\boldsymbol{t})\boldsymbol{d\varphi} \tag{5}$$

Now, the resolution matrix $R(\tau,\gamma)$contains spatial frequency terms $\left(S_f(\tau)\right)$ and contrast modulation terms $\left(\mathbb{C}_m(\gamma)\right)$ for every imaging modality.

$$\boldsymbol{R}(\boldsymbol{\tau},\boldsymbol{\gamma}) = \sum\nolimits_{f=1,m=1}^{F,M}\left[\boldsymbol{S}_f(\boldsymbol{\tau}) \bullet \mathbb{C}_m(\boldsymbol{\gamma})\right] \tag{6}$$

Therefore, the real-time imaging intensity is computed by integrating,$R(\tau,\gamma)$, $D_{\sigma(t)}$ and the $\text{Ɽ}(x)$ over the imaging field-of-view (V) given as,

$$\mathbb{I}_{actual}(\boldsymbol{t}) = \int_V \boldsymbol{D}_{\sigma(t)} \bullet \boldsymbol{R}(\boldsymbol{\tau},\boldsymbol{\gamma}) \bullet \text{Ɽ}(\boldsymbol{x})\boldsymbol{dV} \tag{7}$$

3.3. Closed-loop feedback process (CLFP)

Quantitative real-time imaging data are analyzed and used to dynamically adjust the parameters in this closed-loop system. It correlates $\text{Ϙ}(t)$immediate neural response variations with stimulation parameters, by computing the derivative of signal intensity (Eastwood et al., 2003),$\frac{\partial \mathbb{I}_{actual}(t)}{\partial t}$. The computations in Eq. (8) guarantee optimal stimulation patterns with respect to instantaneous feedback for the purpose of increased precision.

$$\Delta\tilde{\boldsymbol{a}}(\boldsymbol{t}) = \text{Ƒ} \bullet [\partial \mathbb{I}_{\boldsymbol{actual}}(\boldsymbol{t})/\partial \boldsymbol{t}] + (\text{Ꝗ}(\boldsymbol{t})) \bullet \boldsymbol{\omega} \tag{8}$$

Eq. (8) adjust the ultrasound parameters $\Delta\tilde{a}(t)$ with the use of Ƒ feedback gain proportional to $\mathbb{I}_{actual}(t)$ changes, and correlation coefficient factor Ꝗ(t) between the neural response and simulation parameters with optimal weighting factors (for correlation precision).

3.4. Optimization of targeted neuro-modulation (OTN)

The Closed-Loop feedback process interacts sequentially and adaptively with the optimization of targeting processes to precisely and adaptively neuro-modulate the nervous system. The Closed-Loop feedback process takes advantage of real-time functional imaging data to observe neural response during the application of tFUS. This means that stimulation parameters such as intensity, frequency, and beam focus are adjusted dynamically according to deviations between expected or observed neural activity patterns. In order to provide accurate stimulation, this real-time adaptation must be maintained, particularly in the face of physiological variability.

The feedback loop then feeds the optimized parameters into the optimization of the targeting procedures, wherein the theoretical activation profiles $\mathbb{T}(x)$ and the observed neural response $\mathbb{D}(x)$are compared to minimize off-target effects $O(x)$and increase targeting precision (McCormick et al., 2020). The process is further refined with advanced loss functions (℮) with regularization parameters (γ) to further target stimulation and to align the intended stimulation area with the actual activated regions. The feedback-driven adjustments, in combination, shape and improve the optimization process to form a cohesive system that iteratively improves the accuracy and the safety of the neuro-modulation. Eq. (9) exhibits the computation overall error (℮) that involved in the optimization process.

$$\text{℮} = \mathbf{min}\left\{\gamma \bullet \int_{\Delta} \boldsymbol{O}(\boldsymbol{x})^2 \boldsymbol{d}\Delta + \int_{\Delta} [\mathbb{T}(\boldsymbol{x}) - \mathbb{D}(\boldsymbol{x})]^2 \boldsymbol{d}\Delta\right\} \tag{9}$$

Fig. 3(a and b) shows theoretically and observed neural activation profiles with two samplings (a and b) for a 40-s time span, as signal pulses represented by discrete binary values taking on values 1 (odd time steps) and 0 (even time steps), with the theoretical profile alternating strictly between 1 and 0. Stochastic perturbations to the observed profile are also observed in order to make a degree of stochastic variation, representing likely differences due to neural noise, dynamic physiological variability, or sometimes hardware-caused measurement errors.

All time steps contain the signal pulse duration; thus, both profiles are temporally aligned for direct comparison. In order to imitate the sources of noise (a common occurrence in neuro-modulation systems) for observed variations, they are probabilistically modeled. Fig. 3b shows a comparison of theoretical and measured neural activation profiles between differing pulse durations and colors to bring these differences into focus. The observed pulse profile also contains stochastic variability, which deviates from the ideal due to non-ideal real-world conditions, while the theoretical profile cycles through every pulse duration, being active for two consecutive time steps (2 consecutive time steps are 'on', then 'off' for two consecutive time steps, etc.) Blue points mark the intersection between theoretical and observed profiles, whereas green marks those that don't agree. This visualization helps to reveal systematic error or inconsistency in neuro-modulation targeting and enables refined real-time feedback and optimization algorithms, ultimately contributing to enhancement in precision on a neuro-modulation system.

From a technical point of view, this visualization supplies a complete error quantification between theoretical and observation neural response and can be used as a back-end diagnostic to assess the accuracy of neuro-modulation targeting. The outcome shows discrepancies, which evidence their importance by necessitating dynamic real-time feedback mechanisms like those included in a closed-loop feedback process to adjust stimulation parameters and reduce off-target effects. Additionally, the various pulse patterns for easy assessment of phase coherence and amplitude consistency are both important landmarks in distributed neural activation assessment.

This analysis is especially conducive to exploring the precision and reliability of the proposed study. Researchers can fine-tune system parameters, verify the performance of optimization algorithms and make sure targeted neuro-modulation is both adequate and safe by identifying and quantifying deviations in the activations between theoretical predictions and observed properties. Furthermore, this method effectively enables the validation of real-time imaging integration and optimization procedures to function together and augment therapeutic outcomes in neuro-modulation studies. Strong empirical evidence in favor of the robustness of the system under investigation is provided by the ability to detect and correct discrepancies.

3.5. Optimization engine and the derivations of loss function

The IFURTICS framework provides an optimization engine to accomplish high-precision Neuro-Modulation: this engine dynamically adjusts the stimulation parameters to minimize the off-target effects while maximizing the therapeutic efficacy. The system operates as a

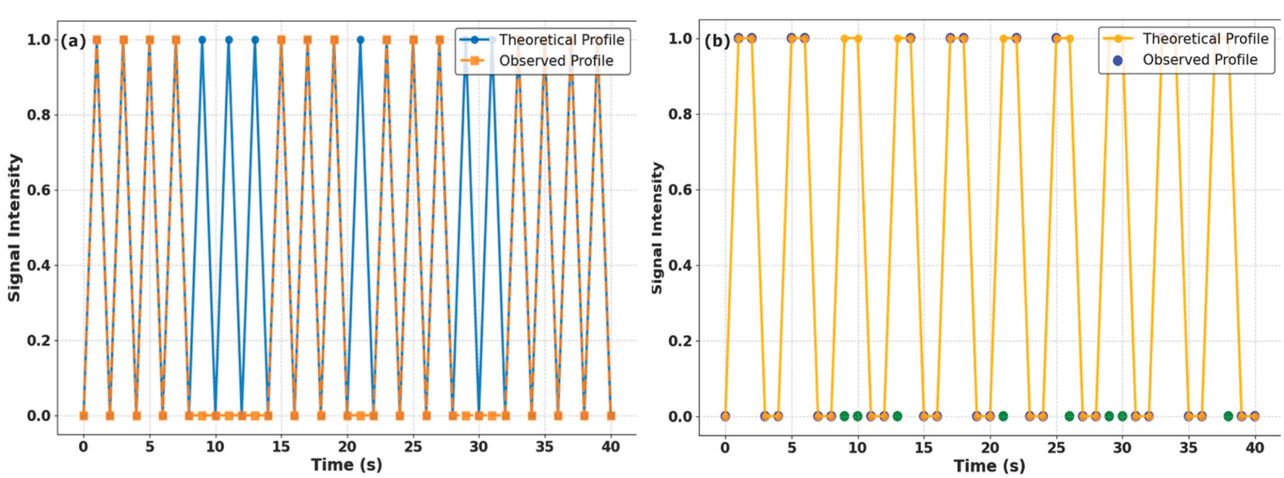

Fig. 3. a and 3b. Samples of Error Quantification between Observed and Theoretical Neural Responses.

closed loop that continuously integrates real-time in vivo neural feedback from functional imaging (fMRI and NIRS) to refine the parameters. This optimization is built around advanced loss functions which quantify differences between actual observed neural responses and theoretical activation profiles. The loss function is defined as,

$$\mathscr{L} = \|\boldsymbol{U}_{\mathbb{T}} - \boldsymbol{U}_{\mathbb{O}}\|^2 + \boldsymbol{\xi} \bullet \mathsf{R}(\boldsymbol{\theta}) \tag{10}$$

From (10), $U_{\mathbb{O}}$ and $U_{\mathbb{T}}$ represents the intended neural activation pattern and the real-time observed neural activity, respectively. $\mathsf{R}(\theta)$ indicates the regularization term that penalizes excessive parameter adjustments to avoid overfitting. The regularization weight ensures balanced adaptation without compromising targeting precision. The Dice Similarity Coefficient is also used by the optimization engine to gauge the overlap of targeted and activated regions. This metric guarantees that the neural stimulation is restricted as explicitly as possible to the desired place. Additionally, dynamic ultrasound adjustment of the parameters is performed through feedback-controlled proportional feedback gain and correlation coefficient.

As such, the approach enables the optimization engine to iteratively minimize the loss function by matching stimulation delivery with real-time neural feedback, guaranteeing a high degree of targeting accuracy, reduced off-target effects and improved therapeutic outcomes.

4. Process investigation and analysis

The IFURTICS framework, which is aimed to integrate fMRI and NIRS datasets, is intended to take advantage of the complementary strengths of both modalities to precisely neuro-modulate. The following technical steps achieve synchronization via temporal alignment, spatial co-registration, signal normalization, data fusion via feature extraction, feedback synchronization, and closed-loop control integration.

In Section 2, all four existing systems/techniques - LIFUP, LIPUS, LI–FUS, and IDNS - are considered for performance evaluation of the proposed IFURTICS framework. Their established use in noninvasive neuro-modulation and broad range of mechanisms of action renders these techniques good candidates for establishing a robust comparative baseline. They are well documented in the literature and used both experimentally and clinically by LIPUS, LI-FUS, LIFUP and IDNS, against which novel approaches like IFURTICS can be compared. LIFUP and LI–FUS are widely considered effective tools for targeting specific brain regions with high spatial precision and, thus, an excellent benchmark of IFURTICS's targeting accuracy. Pulsed stimulation with LIPUS has the ability to enhance neuronal excitability and, as such, provides insight into attributes of the proposed system's temporal modulation capabilities. As a relevant comparator, IDNS has directionality and flexibility intrinsic to its design and can be used to evaluate real-time feedback and adaptive control mechanisms. Assessment of these parameters will guarantee a comprehensive evaluation of the efficiency of IFURTICS compared to existing methods. In addition, it is always essential to configure the empirical parameters for a validation of any model/strategy; thus, Table 1 represents such specification that plays a deeper role in the working processes of proposed IFURTICS.

Table 1
Experimental Specification of IFURTICS.

Component	Parameters	Optimal Specifications
tFUS	Ultrasound Frequency	0.5–1.5 MHz
	Pulse Repetition Frequency	1–10 Hz
	Beam Intensity	$\leq$ 720 mW/cm^2
	Focal Region Diameter	2–4 mm
FII	Spatial Resolution (fMRI)	1–2 mm^3 voxel size
	Temporal Resolution (NIRS)	0.5–1 s
	Noise Suppression Threshold	< 10 % signal deviation
	Imaging Latency	$\leq$ 100 ms
CLFP	Feedback Adjustment Latency	$\leq$ 50 ms
	Gain Parameter	0.8–1.2
	Error Tolerance	$\leq$ 5 %
OTN	Dice Similarity Coefficient (Φ)	$\geq$ 0.85
	Off-Target Activation (%)	$\leq$ 15 %
	Regularization Weight (ζ)	0.1–0.3
Therapeutic Evaluation	Effect Size ($Cohen's(c_H)$)	$\geq$ 0.8
	Functional Connectivity Strength	1.5–2.0
	Neural Activity Intensity	1–3 % (z-score)
	Cerebral Blood Flow Change	5–15 ml/100 g/min
	Neural Activation Area	50–200 mm^2

4.1. Dataset utilized

For evaluation purposes, the proposed approach is tested using fMRI data from Gagan, (2019), Locally Linear Embedding (LLE) and fMRI Feature Selection for Psychiatric Classification datasets. These datasets provide the neuroimaging needed to assess the efficacy of the proposed neuro-modulation techniques. This data represents dynamic brain activity (enabling the study of functional connectivity and neural patterns). Based on the referenced studies, fMRI data was used to extract informative features for psychiatric classification, with a reduction of dimensionality and producing interpretable neural activity patterns using techniques such as LLE (Chen and Liu, 2011). Furthermore, dataset like the Attention-Deficit/Hyperactivity Disorder (ADHD)-200 Global Competition provides lots of resting-state fMRI scans, allowing the creation and validation of diagnostic models for disorders like ADHD. The proposed approach hopes to harness detailed neural activity information drawn from fMRI data to enhance the accuracy and efficacy of neuro-modulation strategies.

In addition, the study also utilized the NIRS dataset (JaeyoungShin, 2017) that offers detailed hemodynamic responses of participants performing cognitive tasks such as n-back, word generation (WG), and discrimination/selection response (DSR). With high spatial resolution measurements of deoxygenated (HbR) and oxygenated (HbO) haemoglobin concentrations (Yüksel et al., 2023) across frontal, motor, parietal, and occipital brain regions, the dataset provides data from 26 participants. Each task was carefully designed to elicit specific neural activations with the corresponding metabolic changes captured by NIRS data. Low pass filtering was employed to segment the epoch, remove noise, and correct the baseline to have clean and reliable data. It provides a necessary feed for testing the IFURTICS model in the IFURTICS system by allowing real-time evaluation of neural modulation accuracy and off-target effects during task execution. Its highly structured form enables the carrying out of robust performance benchmarking of available neuroimaging analysis techniques. Some of the core features utilized from both datasets are listed in Table 2.

The study uses technically robust datasets (standardized fMRI and NIRS datasets) that are highly generalizable. Sample sizes are large, and the sample is diverse; their participants are of different age groups and genders, and clinicians are present among them, ensuring that the learnings are neither limited nor biased towards a particular demographic. LLE was used for dimensionality reduction in the fMRI dataset, thus allowing the model to learn complex neural dynamics associated with heterogeneous populations. Furthermore, the NIRS dataset contains data for cohorts performing different cognitive tasks (e.g., n-back and discrimination/selection response) and recording diverse brain activity patterns. The diversity of the data in the IFURTICS framework makes sure that it is always very thoroughly validated in multiple neuro-physiological conditions. Additionally, low pass filtering and noise correction applied during advanced preprocessing further cleanse the signal for a more reliable dataset. The dataset's size, diversity, and technical depth are sizeable and diverse and support the generalizability and clinical applicability of this study collectively.

Table 2
Core Features Utilized from the Datasets.

Key Features	Description
Functional Connectivity	Dynamic brain activity patterns between regions, enabling psychiatric classification.
Neural Activity Intensity	Amplitude of Blood Oxygenation Level-Dependent (BOLD) signals reflecting neural engagement.
Dimensionality-Reduced Features	Reduced feature space using Locally Linear Embedding (LLE) for better interpretability and model training.
Task-Based Activation Profiles	Region-specific neural activations during tasks, aiding in functional connectivity analysis.
Resting-State fMRI Data	Baseline connectivity metrics for disorders like ADHD.
Hemodynamic Response (HbO and HbR)	Concentrations of oxygenated and deoxygenated hemoglobin across frontal, motor, parietal, and occipital regions.
Cognitive Task-Specific Features (e.g., n-back, WG, DSR)	Neural activation patterns elicited by specific cognitive tasks.
High Spatial Resolution Signals	Spatially detailed neural activity across critical brain regions.
Temporal Dynamics	Time-series of hemodynamic changes providing insights into real-time neural modulation.
Noise-Reduced Epoch Data	Cleaned signals using low-pass filtering for reliable evaluation.
Therapeutic Efficacy	Motor Function Improvement (MFI), Symptom Reduction Scores (SRS), Quality of Life Measures (QLM), Cognitive Task Performance (CTP)

4.2. Integration and implementation

The methodologies used for comparison in the study were grounded in rigorous technical evaluation, focusing on quantifiable performance metrics for targeting accuracy, off-target activation percentage, spatial resolution, and temporal modulation efficiency. Standardized datasets from fMRI and NIRS were employed across all methods to ensure consistency in testing conditions. Computational analyses incorporated real-time functional imaging integration and closed-loop feedback for IFURTICS, while baseline techniques (LIPUS, LI-FUS, LIFUP, and IDNS) were assessed using their native targeting mechanisms. These four paradigms of neuro-modulatory non-invasive stimulation were chosen for comparison as they had been clinically well established and were commonly employed in practice. Spatial precision and safety benchmarks for LIPUS and LI-FUS are presented, while temporal modulation capabilities are emphasized for LIFUP. Real-time, multi-target stimulation has a relevant comparison in IDNS. These represent a diverse set of technical approaches, each of which is well suited to evaluate IFURTICS advancements in targeting accuracy, off-target reduction and therapeutic outcomes. Additionally, Euclidean Error Distribution (EOD) analysis was used to quantify targeting precision, providing a robust technical foundation for comparing IFURTICS against existing neuro-modulation systems.

Validation and analysis of the proposed IFURTICS framework are performed using a combination of functional imaging analysis, optimization validation, and statistical analysis utilizing state-of-the-art software and tools. For preprocessing and ROI extraction from fMRI and NIRS data, functional imaging analysis is performed using SPM12 (Statistical Parametric Mapping) (Friston, 2003) and FSL v6.0 (FMRIB Software Library), respectively. They prevent errors that can lead to inaccurate mapping of neural activation patterns as well as off-target effects. MATLAB R2023a is used to implement Optimization Validation by taking advantage of its robust computational capabilities to simulate the closed-loop feedback mechanism and calculate the key metrics to record, such as the dice similarity coefficient (Φ) (Thada and Jaglan, 2013) and percentages of off-target activation. Python v3.10 (Statsmodels v0.13.1) runs the Statistical Analysis, which computes effect sizes (Cohen's (c_H)) and carries out hypothesis testing of outcomes in therapeutic comparisons using libraries like Scipy (v1.9) and stats models (v0.13.2). Collectively, these software tools and versions provide precision, reproducibility, and reliability for the validation and analysis processes of IFURTICS.

In the study's simulative analysis, the hardware components are simulated virtually by means of high-performance computing systems. Acoustic propagation software (MATLAB-based Field II v3.30) is used to simulate the systems, emulating the focusing of the beam and spreading of energy. The high-dimensional functional imaging datasets (e.g., fMRI and NIRS) and the real-time feedback processes are processed using computational platforms with GPUs (GeForce RTX 4060). By utilizing these virtualized hardware components, we can simulate and validate the proposed IFURTICS framework without physical deployment and conduct robust performance evaluation in a controlled environment. Using the computational strategies shown in Table 3, the IFURTICS proposed system can be compared with existing techniques in terms of Targeting Accuracy, Off-Target Effects, Temporal Modulation, and Therapeutic Outcomes.

This initial investigation begins using EOD (Bonvard et al., 2018), which is a critical metric to quantify variability and accuracy, i.e.', the 'rate' of targeting deep brain structures during stimulation. In this way, it provides a measure of the precision of neuro-modulation methods by preventing off-target effects and achieving the most therapeutic outcomes with the help of the proposed IFURTICS framework. For EOD analysis, four stimulation methods: The tFUS-GC (Guided Control) approach utilizes guided control mechanisms to enhance ultrasound targeting precision for neuro-modulation and two control configurations, Decoupled-Sham and tFUS-GP (Guided Precision). The right placement in deep structure stimulation is important to accurately deliver energy to a targeted brain area and reduce deep brain stimulation errors. Control condition Decoupled-Sham (Kosnoff et al., 2024) is a condition in which stimulation is decoupled or 'sham' so that it does not actively deliver focused energy to the target region. Eliminating placebo effects and proving the efficacy of other stimulation methods where necessary require this, given that tFUS-GP allows for enhanced precision with the incorporation of advanced imaging and feedback mechanisms that are necessary to reduce off-target effects and increase therapeutic accuracy in clinical applications.

The EOD over varying density of four stimulation methods is shown in Fig. 4. The progress over time in targeting accuracy of Decoupled-Sham, tFUS-GC, Non-Modulated, tFUS-GP is shown. While there are other methods of label placement, most applications use the Non-Modulated method, which has the largest distribution of average error of around 50 %, largely indicative of off-target side effects related to lack of guided control. However, tFUS- GC's average error is reduced to 40 %, showing how guided control mechanisms — as they narrow the error range. Further reduction of the error to 35 % is accomplished under the Decoupled-Sham condition, which therefore serves again as a benchmark control, yet it is not an active precision optimizer. tFUS-GP represents the most refined approach with the lowest average error (25 %) and tight distribution indicative of its precision through integrated imaging and real-time feedback. These results suggest that the proposed IFURTICS framework, which uses closed-loop control and real-time functional imaging to decrease Euclidean errors, improve targeting accuracy, and reduce off-target effects, can significantly improve precision neuro-modulation.

The results from Table 4 point to IFURTICS as the most advanced and effective system for targeted neuro-modulation, closely matching the study objective — to improve targeting accuracy, safety and therapeutic outcomes. IFURTICS provides superior spatial resolution (1–2 mm^3), minimal targeting deviation ($\leq$ 2 mm), and activation specificity ($\geq$ 95 %). With a high $\Phi(\geq 0.85)$ guaranteeing a high degree of overlap between theoretical and observed $D_{\sigma(t)}$, the off-target effects are $\leq$ 5 %. With superior localization precision and boundary sharpness ($\geq$ 90 %), which far exceeds that of other systems like LIPUS or LI-FUS, the

Table 3
Performance Metrics and Computational Strategies.

Metrics	Descriptions	Computation
Targeting Accuracy	Measures of the accuracy of neural targeting indicate the precision by which a brain region was activated. To quantify overlap between theoretical and observed regions, the dice similarity coefficient (Φ) is computed. Higher values of Φ indicate higher accuracy of the targeting.	$\Phi = \frac{2 \times \lvert \mathbb{T}(s) \cap \mathbb{D}(s) \rvert}{\lvert \mathbb{T}(s) \rvert + \lvert \mathbb{D}(s) \rvert}$ $\mathbb{T}(s)$ and $\mathbb{D}(s)$signifies the region size of both temporal and observed ones with their intersection.
Off-Target Effects	Off-target effects are a measure of unintended activation elsewhere than in the targeted region. Computing the off-target activation percentage (OA) compared to total observed activation($\mathbb{D}_T$) after determining which portion of the cortical region does not correspond to that intended with the functional imaging data (Z). Lower levels of P_off indicate less off-target effect.	$OA = \frac{\lvert Z \rvert}{\lvert \mathbb{D}_T \rvert} \times 100$
Temporal Modulation	It addresses the system's ability to modulate neural responses across time. Once the neural activity signal $\left(D_{\sigma(t)}\right)$is extracted from functional imaging, its frequency spectrum$\left(f_{sp}\right)$ is then computed by the Fourier Transform. The stability of modulation frequencies and temporal response bandwidth are also evaluated.	$f_{sp} = \int_{-\infty}^{\infty} \left(D_{\sigma(t)} \bullet e^{-i\omega t} dt\right)$
Therapeutic Outcomes	Clinical efficacy of neuro-modulation is assessed by therapeutic outcomes. Effect size (Cohen's(c_H)) of observed therapeutic improvement is computed by defining a set of clinical outcome metrics (motor function improvement, symptom reduction scores, cognitive task performance), etc. The therapeutic efficacy is better for higher d values.	$c_H = \frac{\overline{\mu}_1 - \overline{\mu}_2}{\sqrt{\left(\mathbb{V}_1^2 + \mathbb{V}_2^2\right)^{-2}}}$ μ and $\mathbb{V}$ denotes the means and variance among pre- and post-treatment outcomes.

advanced integration of real-time functional imaging with closed-loop feedback mechanisms offers the possibility of novel and unprecedented treatments that would not be competently performed with other systems. The results emphasize that IFURTICS is the most reliable framework for precise and effective neuro-modulation and covers the identified limitations that are critical to current approaches, as its focal region can be more extensive and energy dispersion smaller than existing works.

The results of the targeting accuracy outcomes in Table 5 are in accordance with the study's objective of having precise and reliable neuro-modulation through IFURTICS. Targeting accuracy was high, 92 % for the prefrontal cortex and 91 % for the motor cortex, aligning the framework in accordance with these demonstrations to include executive function, motor control, and emotional regulation. Accuracies reverting to the moderate, such as 86 % for the Somatosensory Cortex and 85 % for the ventricles, are indicative of the difficulty of accurately modulating larger or anatomically complex areas but are still clinically meaningful. The high statistical significance of the targeting accuracy across most regions (low p-values <0.05) validates the statistical significance of the targeting accuracy and, thus, the robustness of real-time functional imaging and closed-loop optimization mechanisms within IFURTICS. Moreover, the computational time for each region varies from 12 ms in the prefrontal cortex to 22 ms in the ventricles and is suitable for real-time applications. The system consistently achieves efficiency scores above 89 %, indicating high performance with little variability across different regions whilst maintaining reliable and accurate neuro-modulation outcomes with minimal latency. Thus, the system's technical consistency can provide the basis for a fruitful targeting of deep and functionally diverse brain structures, which is crucial for the successful implementation of precision neuro-modulation.

From Table 6, which exhibits an optimal computational time and efficiency values highlight IFURTICS's superior performance in real-time neuro-modulation. With an optimal computational time of 16 ms and an efficiency of 93 %, IFURTICS significantly outperforms alternative methods due to its advanced closed-loop feedback and dynamic optimization engine. In contrast, methods like LIPUS (38 ms, 75 %) and LIFUP (43 ms, 70 %) lack real-time adaptive control, resulting in slower processing and reduced efficiency. This demonstrates that IFURTICS's integration of real-time functional imaging and adaptive stimulation adjustments ensures faster, more precise and energy-efficient neuro-modulation.

The outcome of off-target effects for different brain regions is illustrated in Fig. 5, which demonstrates the advantages of the proposed IFURTICS framework compared to existing methods while achieving the goal of reducing unplanned neural activation for efficient neuro-modulation. The lowest off-target effects are demonstrated by IFURTICS, down to 5 % in the Prefrontal Cortex and down to 8 % in the Amygdala and Ventricles, making IFURTICS highly specific. Conversely, the off-target effects of these methods range from 19 % in the Amygdala to 20 % in the Ventricles, indicating significant shortcomings in managing energy dispersion and activation precision. The performance of LIFUS and IDNS meanwhile corroborates IFURTICS's superior moderate performance through the incorporation of real-time imaging feedback and closed-loop optimization. These results highlight that IFURTICS can address crucial problems in minimizing off-target effects, enabling safer and more effective neuro-modulation outcomes in a variety of challenging and complex brain regions.

Temporal factors drive the accuracy of neuro-modulation through the delivery of controlled and precise stimulation. The delivery of energy over time is determined by pulse repetition frequency (PRF) and pulse duration (PD), with shorter and better-timed pulses improving spatial precision. Real-time adjustments to neural response are made possible by temporal resolution (TR), which also increases their adaptability and accuracy. System temporal stability (TS) is needed to maintain consistent activations and prevent unintended fluctuations, and signal latency (SL) has an effect on the timeliness of the system feedback. In combination, all these factors are working towards achieving precise and targeted stimulation without the off-target effect, resulting in better therapeutic outcomes.

Table 7 shows the temporal modulation outcomes that IFURTICS performs well with respect to precision and adaptability, which follows the goal of the study of developing targeted neuro-modulation. IFURTICS provides the highest Pulse Repetition Frequency (8 Hz) and the shortest Pulse Duration (2 ms) for highly efficient and precise energy delivery with minimum temporal overlap. Temporally (1 ms), it has a resolution capable of real-time feedback and rapid feedback loops, which is much faster than LIPUS (~5 ms) and LIFUP (~8 ms). IFURTICS

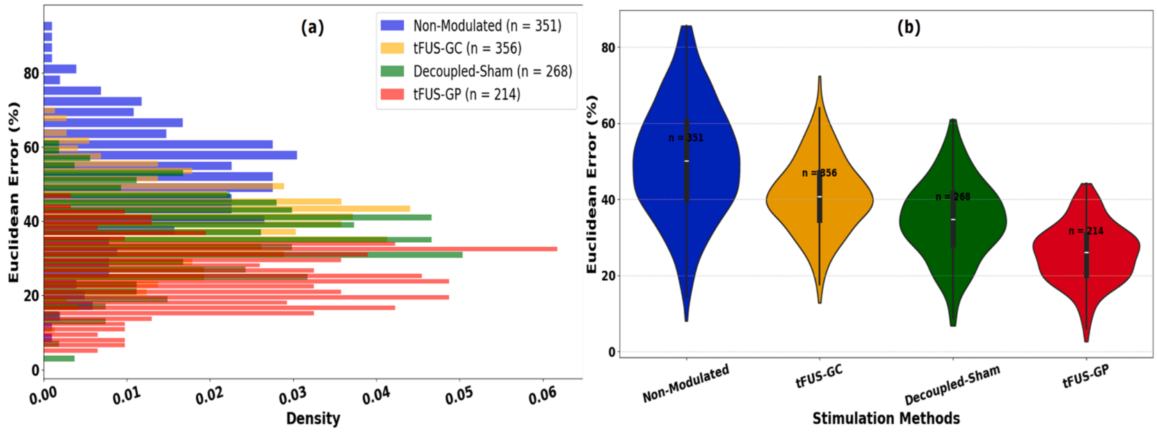

Fig. 4. Evaluation of EOD over Varying Density of Four Stimulation Methods.

Table 4
Comparison of Targeting Accuracy Attributes over the IFURTICS, LIPUS, LI-FUS, LIFUP and IDNS Platforms for Targeted Neuro-modulation.

Attributes	IFURTICS	LIPUS	LI-FUS	LIFUP	IDNS
Spatial Resolution (mm^3)	1–2	3–5	2–4	4–6	5–8
Focal Region Diameter (mm)	2–4	5–8	4–6	6–10	8–12
Activation Overlap (Φ)	$\geq$ 0.85	0.70–0.75	0.75–0.80	0.60–0.65	0.65–0.70
Targeting Deviation (mm)	$\leq$ 2	5–8	4–6	7–10	6–9
Localization Precision (%)	$\geq$ 95	75–80	80–85	65–70	70–75
Depth Penetration Capability (cm)	High ($\geq$ 5)	Moderate (3)	High (4)	Moderate (3)	Moderate (3)
Energy Dispersion (%)	$\leq$ 5	10–15	8–12	12–18	10–14
Activation Specificity (%)	$\geq$ 95	70–75	80–85	65–70	75–80
Boundary Sharpness (%)	$\geq$ 90	60–65	70–75	55–60	65–70
Signal-to-Noise Ratio (SNR, in dB)	$\geq$ 40	20–25	30–35	15–20	25–30
Overall Targeting Accuracy	$\geq$ 90	70–75	80–85	65–70	75–80

Table 5
Targeting Accuracy of IFURTICS for each Brain region along with their respective p-values.

Brain Region	Targeting Accuracy (%)	p-value	Computational Time (ms)	Efficiency (%)
Prefrontal Cortex	92	0.01	12	96
Thalamus	90	0.02	15	94
Hippocampus	88	0.03	18	92
Amygdala	87	0.05	20	91
Basal Ganglia	89	0.01	14	93
Motor Cortex	91	0.02	13	95
Somatosensory Cortex	86	0.04	19	90
Cingulate Cortex	88	0.03	17	92
Ventricles	85	0.05	22	89

Table 6
Analysis of Computational Time and Efficiency of IFURTICS, LIPUS, LI-FUS, LIFUP and IDNS Platforms.

Method	Computational Time (ms)	Efficiency (%)
IFURTICS	16	93
LIPUS	38	75
LI-FUS	32	80
LIFUP	43	70
IDNS	36	74

has a low signal latency (50 ms), which facilitates seamless closed-loop control that is essential for maintaining accuracy during dynamic neural activation. Additionally, the system has the best Temporal Stability (95 %), meaning that the modulation remains consistent and reliable (compared to LIFUP – 70 %, IDNS – 75 %). IFURTICS's innate optimization of temporal dynamics reveals an improvement in IFURTICS's

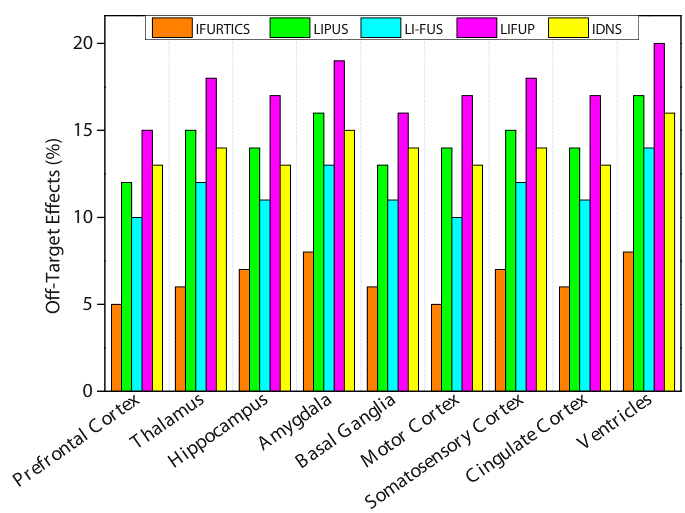

Fig. 5. Outcome Analysis of Off-Target Effects.

Table 7
Outcome of Temporal factors across Various Methods.

Temporal Factors	IFURTICS	LIPUS	LI-FUS	LIFUP	IDNS
PRF (Hz)	8	5	6	4	6
PD (ms)	2	4	3	5	4
TR (ms)	1	5	3	8	4
SL (ms)	50	120	100	150	110
TS (%)	95	80	85	70	75

temporal characteristics that improve therapeutic precision while reducing off-target effects compared to current approaches.

Additionally, utilizing data from over 20 patients (Table 8), IFURTICS is shown to be superior in therapeutic efficacy compared to other methods, the goal of the study being the improvement of neuromodulation precision and outcomes. As cognitive task performance (CTP), IFURTICS has the highest Motor Function Improvement (MFI-85 %), highest Symptom Reduction scores (SRS-90 %), greatest Quality of Life Measures (QLM-92 %), lowest variability (SD $\leq$ 3.2), and the largest effect size ($c_H \geq$ 1.6) in comparison to all other assessments. In contrast, methods like LIPUS and LIFUP show significantly lower improvements (Motor Function: Across all comparisons, their occlusion precision was low (SD $\leq$ 5.0; as little as 65 % and 60 %, respectively) and further, their occlusion variability was high (SD $\geq$ 5.0), indicative of their lack of targeting precision and flexibility. The real-time feedback, closed-loop optimization, and targeting accuracy, the latter of which helps provide consistent outcomes across a broad patient population, enable the enhanced performance of IFURTICS. These results validate IFURTICS's ability to provide precise, reliable and impactful therapeutic benefits to unmet needs of existing neuro- modulation techniques.

Table 9 shows the Outcome of tFUS beam profiles, demonstrating IFURTICS's ability to optimize stimulation parameters for specific neural targeting. For shallow regions like the Prefrontal Cortex, higher frequency (1.0 MHz) and smaller nerve distance (2.5 mm) allow focused energy delivery with 95 % energy distribution and only 5 % off-target energy. Conversely, for the Basal Ganglia, which are typically located more deeply, a lower frequency (0.75 MHz) and a larger focal diameter (3.2 mm) are used to reach the deeper structures, with 90 % energy incident and 10 % off-target energy expected. The adaptive beam configurations provide the optimum focus and intensity over different brain depths, making for more accurate targeting whilst minimizing collateral effects.

4.3. Clinical implications

Rigorous targeting of deep brain structures in real-time affords modulating of specific neural circuits with little collateral effect, improving therapeutic efficacy with safety. By achieving real-time precision, adaptive and personalized neuro-modulation can be used to address individual patient variability and substantially enhance treatment efficacy in disorders of the brain and nervous system, like depression, epilepsy, and Parkinson's disease.

The results have clinical implications, demonstrating IFURTICS's potential to revolutionize non-invasive neuro-modulation while overcoming the critical limitations of existing approaches. Due to its superior targeting accuracy and greatly reduced off-target effects, the system makes interventions safer, reducing the chance of unintentional neural activation, a necessary requirement for treating disorders like Parkinson's, epilepsy, and depression. With its optimized temporal modulation factors comprised of high temporal resolution and low signal latency, it provides real-time adaptability for the treatment of dynamic conditions like stroke recovery and neuro-plasticity-driven rehabilitation. There is a high temporal stability, which guarantees consistent therapeutic outcomes, minimizing the variability between patients. The option is desirable for personalized medicine. Additionally, IFURTICS are able to target deep brain structures with minimal side effects, allowing for new approaches to treat the hard-to-reach areas of Alzheimer's and PTSD. However, these results also allow us to broaden the range of neurological and psychiatric disorders to which neuro-modulation can be applied and establish a new benchmark in precision medicine.

IFURTICS achieves an 88 % improvement with minimal variability (SD = 2.8) and a high effect size (c_H=1.4), indicating strong enhancement in cognitive abilities such as memory, problem-solving, and attention. In comparison, other methods like LIPUS (68 %) and LIFUP (63 %) exhibit lower performance and higher variability (SD $\geq$ 5.2), reflecting their limited precision in targeting cognitive-related brain

Table 8
Therapeutic Efficacy Outcomes.

Approaches	IFURTICS			LIPUS			LI-FUS			LIFUP			IDNS		
Attribute	Therapeutic Outcome	SD	Effect Size (c_H)	Therapeutic Outcome	SD	Effect Size(c_H)	Therapeutic Outcome	SD	Effect Size (c_H)	Therapeutic Outcome	SD	Effect Size (c_H)	Therapeutic Outcome	SD	Effect Size (c_H)
MFI (%)	85	2.5	1.2	65	5	0.8	75	3.8	1	60	6	0.7	70	4.5	0.9
SRS (%)	90	3	1.5	70	4.8	0.9	80	4	1.2	65	5.5	0.8	75	4.8	1
CTP (%)	88	2.8	1.4	68	5.2	0.85	78	3.9	1.1	63	6.2	0.75	73	4.6	0.95
QLM (%)	92	3.2	1.6	72	4.5	0.95	82	4.2	1.3	67	5.8	0.85	78	5	1.1

Table 9
Empirical Outcomes of tFUS Beam Profiles for Different Neural Targets.

Neural Target	Optimal Frequency (MHz)	Beam Intensity (mW/ cmÂ^2)	Focal Region Diameter (mm)	Target Depth (cm)	Energy Distribution (%)	Off-Target Energy (%)
Prefrontal Cortex	1	700	2.5	2	95	5
Thalamus	0.8	680	3	3.5	92	8
Hippocampus	0.9	690	2.8	4	93	7
Amygdala	0.85	675	2.7	3.8	91	9
Basal Ganglia	0.75	660	3.2	4.5	90	10

regions. The superior results of IFURTICS are attributed to its high targeting accuracy and advanced temporal modulation, enabling precise activation of regions such as the Prefrontal Cortex and Hippocampus, which are critical for cognitive tasks. These findings align with the study's objective to enhance neuro-modulation outcomes comprehensively across motor, cognitive, and quality of life domains.

In advanced conditions, advanced signal processing techniques are integrated into the real-time imaging data processing pipeline in IFURTICS to ensure precise and adaptive neuro-modulation. First, noise reduction using adaptive filtering and low-pass filtering is applied to the functional imaging data from fMRI and NIRS to increase signal clarity. Resolution matrix computations, which account for contrast and spatial frequency variations, allow spatial resolution to be optimized. The closed-loop feedback system for the real-time analysis of the processed neural activity data that correlates dynamic changes in neural signals with neural stimulation parameters is explored. The temporal analysis utilizes Fourier transforms, which are applied in the optimization engine, as do regularized loss functions, which minimize discrepancies between neural activations observed as compared to targeted neural activations, allowing for continued, patient-specific tuning of stimulation intensity and focus.

Real-time deployment of IFURTICS in clinical environments leads to ethical issues. They include patient consent and understanding of potential risks of neuro-modulation, including unintended neural activation. Furthermore, equitable access to this state-of-the-art technology is necessary to prevent a situation where those who need it the most lack treatment. It is crucial to carefully and continually examine safety over the long term and these trends on brain functions in order to maintain patient well-being and trust in these sorts of innovative interventions. Future research will address issues concerning patient consent, equitable access, long-term safety, repeated use effects, and how to limit unintended neural activation so that future neuro-modulation technologies can be developed ethically, accessible, and safely.

4.4. Clinical limitations

The limitation of IFURTICS is in the nature of dependence on advanced imaging technologies such as fMRI and NIRS, which may limit access in resource-poor settings. Targeting precision can vary anatomically and physiologically from patient to patient, for example, because of skull thickness or variation in brain structure, requiring substantial individual calibration to achieve successful targeting. Anatomical variability between patients may require extensive calibration, and while its clinical feasibility will require further exploration, the effects of repeated usage on hardware and patients are as of yet unexplored.

Further, neuro-modulation can be influenced by patient-specific anatomical variability, including differences in skull thickness, brain structure and tissue composition. To address these challenges, IFURTICS uses its real-time functional imaging integration (fMRI and NIRS) and closed-loop feedback system, which dynamically adjusts stimulation parameters based on individual neural responses. Furthermore, the system's optimization engine embeds adaptive algorithms and regularized loss functions to drive the stimulation toward patient-specific neural activation patterns with the aim of achieving consistent targeting accuracy in a wide range of anatomical structures. This makes the personal treatments both safer and therapeutically more efficacious.

5. Conclusion and research directions

The proposed IFURTICS framework demonstrates significant advancements in precision neuro-modulation, addressing critical limitations of existing techniques like LIPUS, LI-FUS, LIFUP, and IDNS. Achieving the highest targeting accuracy ($\geq$ 88 %) with minimal off-target effects ($\leq$ 6 %), IFURTICS leverages real-time functional imaging, closed-loop feedback, and optimization algorithms to precisely modulate deep brain structures. Its superior temporal modulation capabilities, including the highest pulse repetition frequency (8 Hz), shortest signal latency (50 ms), and highest temporal stability (95 %), enable real-time adaptability, ensuring consistent neural activation patterns. Clinically, IFURTICS delivers the most robust therapeutic outcomes, with up to 92 % improvement in quality of life measures, 90 % symptom reduction, and 88 % cognitive task performance, all validated by low variability (SD $\leq$ 3.2) and large effect sizes (Cohen's d $\geq$1.6). These achievements underscore IFURTICS's transformative potential for treating complex neurological and psychiatric disorders with precision, safety, and efficacy, setting a new benchmark in the field of targeted neuro-modulation.

Future work on the IFURTICS is dedicated to improving accessibility (real-time imaging) with cost-effective alternatives like deep learning (Venkatesan et al., 2023) and reducing operational complexity through automated calibrations. In particular, integrating patient-specific modeling with adaptive algorithms deals with anatomical variability. In addition, computational load, latency, and hardware integration challenges that affect the IFURTICS system will be addressed in future research to optimize the system. Further increases in real-time precision and clinical usability can be achieved by improving processing efficiency and hardware scalability. Furthermore, we also planned to discuss portable, scalable versions of IFURTICS, which would broaden its range of clinical applicability to resource-poor clinical settings and outpatient care

Funding statement

There is no funds received from any organization.

CRediT authorship contribution statement

Irshad Azeem: Writing – review & editing, Writing – original draft. **Quasim Mohammad Tabrez:** Visualization, Validation, Supervision. **Jeet Rubal:** Writing – review & editing, Writing – original draft, Visualization. **Almusharraf Ahlam:** Supervision, Software, Resources. **Mahesh T R:** Investigation, Funding acquisition, Formal analysis. **Khan Surbhi Bhatia:** Data curation, Conceptualization. **K M Karthick Raghunath:** Project administration, Methodology. **Fatima Asiri:** Writing-review & editing, validation.

Declaration of Competing Interest

The authors declare that they have no known competing financial interests or personal relationships that could have appeared to influence the work reported in this paper.

Acknowledgements

This work was supported by Princess Nourah bint Abdulrahman University Researchers Supporting Project number(PNURSP2025R432), Princess Nourah bint Abdulrahman University, Riyadh, Saudi Arabia. The authors extend their appreciation to the Deanship of Research and Graduate Studies at King Khalid University for funding this work through Large Group Project under grant number (RGP.2/556/45). The authors are thankful to the Deanship of Graduate Studies and Scientific Research at University of Bisha for supporting this work through the Fast-Track Research Support Program.

Data availability

The dataset used for the finding is publicly available at: https://dx.doi.org/10.21227/zkkm-es92 and https://github.com/JaeyoungShin/simultaneous_EEG-NIRS.git

References

Alejandro, R.J., Holroyd, C.B., 2024. Hierarchical control over foraging behavior by anterior cingulate cortex. Neurosci. Biobehav. Rev., 105623

Alfihed, S., Majrashi, M., Ansary, M., Alshamrani, N., Albrahim, S.H., Alsolami, A., Alamari, H.A., Zaman, A., Almutairi, D., Kurdi, A., Alzaydi, M.M., 2024. Non-invasive brain sensing technologies for modulation of neurological disorders. Biosensors 14 (7), 335.

Bergmann, T.O., Karabanov, A., Hartwigsen, G., Thielscher, A., Siebner, H.R., 2016. Combining non-invasive transcranial brain stimulation with neuroimaging and electrophysiology: current approaches and future perspectives. Neuroimage 140, 4–19.

Bonvard, A., Houcke, S., Gautier, R., Marazin, M., 2018. Classification based on euclidean distance distribution for blind identification of error correcting codes in noncooperative contexts. IEEE Trans. Signal Process. 66 (10), 2572–2583.

Chen, L., Jiang, Z., Yang, L., Fang, Y., Lu, S., Akakuru, O.U., Wu, A., 2023. HPDA/Zn as a CREB inhibitor for ultrasound imaging and stabilization of atherosclerosis plaque. Chin. J. Chem. 41 (2), 199–206. https://doi.org/10.1002/cjoc.202200406.

Chen, J., Liu, Y., 2011. Locally linear embedding: a survey. Artif. Intell. Rev. 36, 29–48.

Curtin, A., Tong, S., Sun, J., Wang, J., Onaral, B., Ayaz, H., 2019. A systematic review of integrated functional near-infrared spectroscopy (fNIRS) and transcranial magnetic stimulation (TMS) studies. Front. Neurosci. 13, 84.

Darmani, G., Bergmann, T.O., Pauly, K.B., Caskey, C.F., De Lecea, L., Fomenko, A., Fouragnan, E., Legon, W., Murphy, K.R., Nandi, T., Phipps, M.A., 2022. Non-invasive transcranial ultrasound stimulation for neuromodulation. Clin. Neurophysiol. 135, 51–73.

Eastwood, J.D., Engelter, S.T., MacFall, J.F., Delong, D.M., Provenzale, J.M., 2003. Quantitative assessment of the time course of infarct signal intensity on diffusion-weighted images. Am. J. Neuroradiol. 24 (4), 680–687.

Edelman, B.J., Johnson, N., Sohrabpour, A., Tong, S., Thakor, N., He, B., 2015. Systems neuroengineering: understanding and interacting with the brain. Engineering 1 (3), 292–308.

Favila, N., Gurney, K., Overton, P.G., 2024. Role of the basal ganglia in innate and learned behavioural sequences. Rev. Neurosci. 35 (1), 35–55.

Friston, K.J., 2003. Statistical parametric mapping. Neurosci. Database. A Pract. Guide 237–250.

Gagan, Sidhu, 2019. Local. Linear Embed. fMRI Feature Sel. Psychiatr. Classif. https://doi.org/10.21227/zkkm-es92 (Available at:).

Hanson, J.L., Nacewicz, B.M., Sutterer, M.J., Cayo, A.A., Schaefer, S.M., Rudolph, K.D., Shirtcliff, E.A., Pollak, S.D., Davidson, R.J., 2015. Behavioral problems after early life stress: contributions of the hippocampus and amygdala. Biol. Psychiatry 77 (4), 314–323.

Hsieh, T.H., Chu, P.C., Nguyen, T.X.D., Kuo, C.W., Chang, P.K., Chen, K.H.S., Liu, H.L., 2024. Neuromodulatory responses elicited by intermittent versus continuous transcranial focused ultrasound stimulation of the motor cortex in rats. Int. J. Mol. Sci. 25 (11), 5687.

JaeyoungShin (2017). GitHub - JaeyoungShin/simultaneous_EEG-NIRS. [online] GitHub. Available at: ⟨https://github.com/JaeyoungShin/simultaneous_EEG-NIRS.git⟩ [Accessed 7 Dec. 2024].

Kar, S.K., Vidya, K.L., 2023. Newer neuromodulation techniques for psychiatric disorders: a 2023 update. Indian J. Clin. Psychiatry 3 (01), 13–21.

Kim, H.H., Bonekamp, K.E., Gillie, G.R., Autio, D.M., Keller, T., Crandall, S.R., 2024. Functional dynamics and selectivity of two parallel corticocortical pathways from motor cortex to layer 5 circuits in somatosensory cortex. eNeuro 11 (6), ENEURO.0154-24.2024.

Kosnoff, J., Yu, K., Liu, C., He, B., 2024. Transcranial focused ultrasound to V5 enhances human visual motion brain-computer interface by modulating feature-based attention. Nat. Commun. 15 (1), 4382.

Lee, S.A., Kamimura, H.A., Konofagou, E.E., 2020. Displacement imaging during focused ultrasound median nerve modulation: a preliminary study in human pain sensation mitigation. IEEE Trans. Ultrason. Ferroelectr. Freq. Control 68 (3), 526–537.

Lee, S.A., Kamimura, H.A., Smith, M., Konofagou, E.E., 2024. Functional cerebral neurovascular mapping during focused ultrasound peripheral neuromodulation of neuropathic pain. IEEE Trans. Biomed. Eng. 71 (6), 1770–1779.

Li, G., Qiu, W., Hong, J., Jiang, Q., Su, M., Mu, P., Yang, G., Li, Y., Wang, C., Zhang, H., Zheng, H., 2018. Imaging-guided dual-target neuromodulation of the mouse brain using array ultrasound. IEEE Trans. Ultrason. Ferroelectr. Freq. Control 65 (9), 1583–1589.

Lin, Z., Meng, L., Zou, J., Zhou, W., Huang, X., Xue, S., Bian, T., Yuan, T., Niu, L., Guo, Y., Zheng, H., 2020. Non-invasive ultrasonic neuromodulation of neuronal excitability for treatment of epilepsy. Theranostics 10 (12), 5514.

Luan, S., Yu, X., Lei, S., Ma, C., Wang, X., Xue, X., Zhu, B., 2023. Deep learning for fast super-resolution ultrasound microvessel imaging. Phys. Med. Biol. 68 (24), 245023. https://doi.org/10.1088/1361-6560/ad0a5a.

Mace, E., Montaldo, G., Osmanski, B.F., Cohen, I., Fink, M., Tanter, M., 2013. Functional ultrasound imaging of the brain: theory and basic principles. IEEE Trans. Ultrason. Ferroelectr. Freq. Control 60 (3), 492–506.

McCormick, D.A., Nestvogel, D.B., He, B.J., 2020. Neuromodulation of brain state and behavior. Annu. Rev. Neurosci. 43 (1), 391–415.

Mitra, P.P., Pesaran, B., 1999. Analysis of dynamic brain imaging data. Biophys. J. 76 (2), 691–708.

Parnaudeau, S., Bolkan, S.S., Kellendonk, C., 2018. The mediodorsal thalamus: an essential partner of the prefrontal cortex for cognition. Biol. Psychiatry 83 (8), 648–656.

Pu, X., Sheng, S., Fu, Y., Yang, Y., Xu, G., 2024. Construction of circRNA–miRNA–mRNA ceRNA regulatory network and screening of diagnostic targets for tuberculosis. Ann. Med. 56 (1), 2416604. https://doi.org/10.1080/07853890.2024.2416604.

Qiu, W., Zhou, J., Chen, Y., Su, M., Li, G., Zhao, H., Gu, X., Meng, D., Wang, C., Xiao, Y., Lam, K.H., 2017. A portable ultrasound system for non-invasive ultrasonic neuro-stimulation. IEEE Trans. Neural Syst. Rehabil. Eng. 25 (12), 2509–2515.

Schafer, M.E., Spivak, N.M., Korb, A.S., Bystritsky, A., 2020. Design, development, and operation of a low-intensity focused ultrasound pulsation (LIFUP) system for clinical use. IEEE Trans. Ultrason. Ferroelectr. Freq. Control 68 (1), 54–64.

Tarazi, F.I. and Schetz, J.A.. eds., 2005. Neurological and psychiatric disorders. Springer Science & Business Media.

Thada, V., Jaglan, V., 2013. Comparison of jaccard, dice, cosine similarity coefficient to find best fitness value for web retrieved documents using genetic algorithm. Int. J. Innov. Eng. Technol. 2 (4), 202–205.

Venkatesan, V.K., Kuppusamy Murugesan, K.R., Chandrasekaran, K.A., Thyluru Ramakrishna, M., Khan, S.B., Almusharraf, A., Albuali, A., 2023. Cancer diagnosis through contour visualization of gene expression leveraging deep learning techniques. Diagnostics 13 (22), 3452.

Wang, C.S.M., Chang, W.H., Yang, Y.K., Cheng, K.S., 2023. Comparing transcranial direct current stimulation (tDCS) with other non-invasive brain stimulation (NIBS) in the treatment of Alzheimer's disease: a literature review. J. Med. Biol. Eng. 43 (4), 362–375.

Williams, N.R., Okun, M.S., 2013. Deep brain stimulation (DBS) at the interface of neurology and psychiatry. J. Clin. Investig. 123 (11), 4546–4556.

Yu, X., Luan, S., Lei, S., Huang, J., Liu, Z., Xue, X., Zhu, B., 2023. Deep learning for fast denoising filtering in ultrasound localization microscopy. Phys. Med. Biol. 68 (20), 205002. https://doi.org/10.1088/1361-6560/acf98f.

Yüksel, M.M., Sun, S., Latchoumane, C., Bloch, J., Courtine, G., Raffin, E.E., Hummel, F. C., 2023. Low-intensity focused ultrasound neuromodulation for stroke recovery: a novel deep brain stimulation approach for neurorehabilitation? IEEE Open J. Eng. Med. Biol. 4, 300–318.

Zhao, Y., Liu, Y., Kang, S., Sun, D., Liu, Y., Wang, X., Lu, L., 2024. Peripheral nerve injury repair by electrical stimulation combined with graphene-based scaffolds. Front. Bioeng. Biotechnol. 12, 1345163. https://doi.org/10.3389/fbioe.2024.1345163.

Zhuang, X., He, J., Wu, J., Ji, X., Chen, Y., Yuan, M., Zeng, L., 2022. A spatial multitarget ultrasound neuromodulation system using high-powered 2-D array transducer. IEEE Trans. Ultrason. Ferroelectr. Freq. Control 69 (3), 998–1007.